Temperature dependence of the polarized Raman spectra of $ZnWO_4$ single crystals

H. Wang and F. D. Medina
Department of Physics, Florida Atlantic University, Boca Raton, Florida 33431

Y. D. Zhou and Q. N. Zhang*
Beijing Polytechnic University, Beijing, China

(Received 8 July 1991; revised manuscript received 30 September 1991)

The 18 vibrational modes expected from group-theoretical analysis have been obtained in the polarized Raman spectra of $ZnWO_4$ single crystals. The six internal modes of the WO_6 octahedra have been assigned. The temperature dependence of the frequencies and linewidths of the internal modes is related to anharmonic terms in the crystal potential.

INTRODUCTION

In recent years, there has been a growing interest in zinc tungstate ($ZnWO_4$) as a possible new material for scintillator,[1,2] laser host,[3] acoustic,[4] and optical fiber[5] applications. It has promise as a material for x-ray scintillators because its luminescence output and afterglow are comparable to or better than those of materials currently in use.[1,2] In addition, zinc tungstate has the advantage of not being hygroscopic, and materials used in its preparation are not toxic and are much cheaper than those used for ($Bi_4Ge_3O_{12}$) BGO, a widely used scintillator material.

In order to replace other materials, however, large single crystals of $ZnWO_4$ of good optical quality are needed. Studies of the optical properties and the Raman spectra of $ZnWO_4$ at room temperature have been reported in the literature.[6,7] In this paper, the temperature dependence of the polarized Raman spectra in various scattering geometries is presented, a complete assignment of the lattice modes is made, and interactions between phonons are discussed.

$ZnWO_4$ has the monoclinic wolframite structure with C_{2h} point-group symmetry and $P2/c$ space group. It has two formula units per unit cell, with lattice parameters $a=4.72$ Å, $b=5.70$ Å, $c=4.95$ Å, and $\beta=90°05'$.[8] The unit cell of $ZnWO_4$ is isomorphic to those of a group of tungstates (Cd, Mg, Ni, Fe, Co, and Mn) that contain octahedral WO_6 groups.[9] Figure 1 shows the nearly regular WO_6 octahedra in the crystalline structure of $ZnWO_4$. The W-O interatomic distance is substantially smaller than that of Zn-O so that, to a first-order approximation, the lattice interactions can be separated into internal vibrations of the octahedra and the external vibrations in which an octahedron vibrates as a unit.

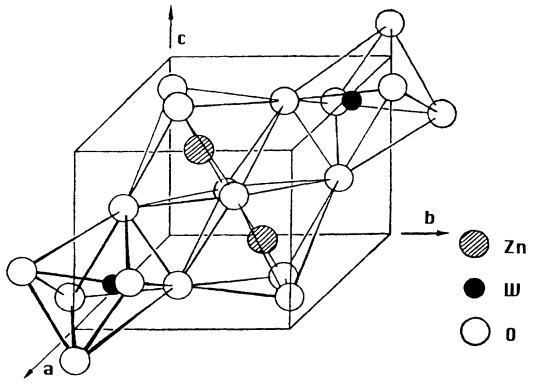

FIG. 1. WO_6 octahedra in the $ZnWO_4$ structure.

A group-theoretical analysis of the $ZnWO_4$ structure yields 36 lattice modes, of which 18 are Raman active: 8 $A_g+10\ B_g$. For the WO_6 octahedra, Table I shows the correlation diagram between the O_h symmetry of an isolated regular octahedron, the C_2 site symmetry that the group has in the crystal, and the $P2/c$ space group symmetry. The degeneracies of the E_g (twofold) and T_{2g} (threefold) are completely removed in the crystal and six modes are expected, $4\ A_g+2\ B_g$. All of these modes are Raman active.

EXPERIMENTAL DETAILS

Single crystals of $ZnWO_4$ were grown in air by a balance-controlled Czochralski technique. Typical growth conditions were a [100] pulling direction, a 3-mm/h pulling rate, a 46-rpm rotational speed, and about a 50-°C/cm temperature gradient.

The $ZnWO_4$ single crystals grown by the conventional Czochralski method were found to be of red-brown color because of oxygen vacancies.[10] Color-free, high-optical-quality single crystals were obtained by using annealing techniques or doping with metallic elements.

The sample used in this work was optically transparent

TABLE I. Correlation diagram for the internal modes of the WO_6 octahedron.

Molecular symmetry (O_h)	Site symmetry (C_2)	Space-group symmetry ($P2/c$)
A_{1g}	A	A_g
E_g	$A+B$	A_g+B_g
T_{2g}	$2\ A+B$	$2\ A_g+B_g$

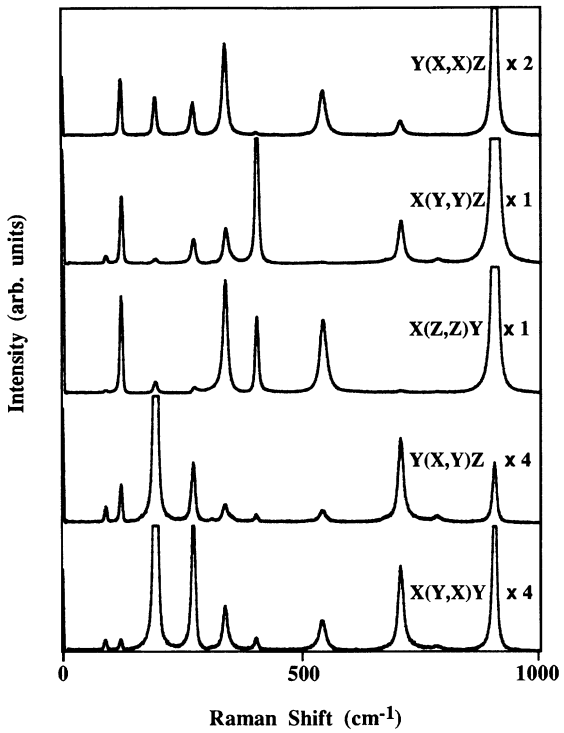

FIG. 2. Raman spectra of $ZnWO_4$ at 292 K showing the A_g modes.

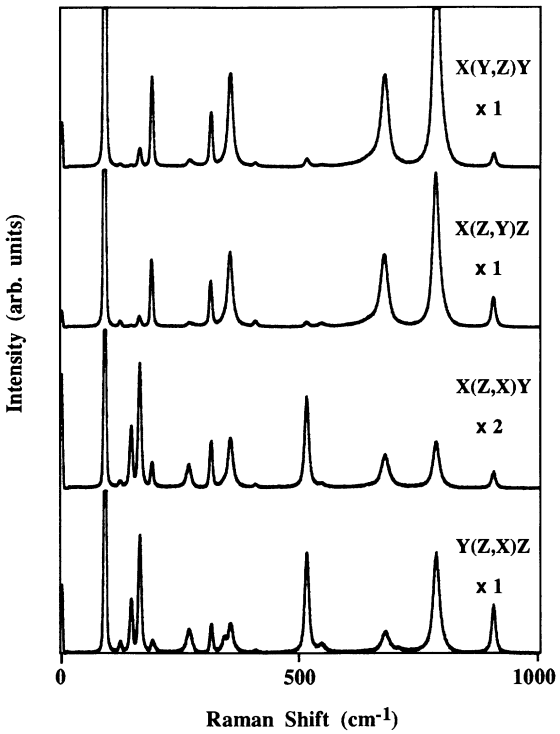

FIG. 3. Raman spectra of $ZnWO_4$ at 292 K showing the B_g modes.

and color free. It was cut and polished into a rectangular block $9\times7\times4$ mm^3 with edges within about 1° of the crystallographic axes, as determined by x-ray diffraction. It was mounted on a sample holder (high-thermal-conductivity copper) attached to the cold finger of a closed-cycle helium refrigerator capable of operating between 10 and 300 K.

The Raman spectra were obtained with the 488-nm line of an argon-ion laser, a Spex 1403 spectrometer, and photon-counting techniques. The spectra were recorded in the region 0–1000 cm^{-1} with a laser beam power of 200 mW. The spectrometer slits were all set at 400 μm, which corresponds to an instrumental resolution of 5.4 cm^{-1}.

TABLE II. Raman-active bands observed in $ZnWO_4$. The asterisks indicate internal modes.

	Modes	Frequency (cm^{-1})		Linewidth[a] (cm^{-1})		Mode symmetry	
		14 K	292 K	14 K	292 K		
*	1	907.5	906.8	5.2	8.3	A_g	
*	2	787.3	785.9	6.0	15.1		B_g
*	3	709.0	709.1	6.6	12.9	A_g	
	4	676.9	678.7	9.1	18.7		B_g
	5	550.0	546.4	5.9	14.6	A_g	
	6	517.5	515.3	3.6	8.9		B_g
*	7	408.0	406.9	3.6	10.2	A_g	
	8	357.2	355.4	3.6	11.1		B_g
*	9	342.5	341.8	3.6	9.6	A_g	
	10	315.9	314.6	1.5	4.8		B_g
	11	277.0	274.4	2.6	8.1	A_g	
	12	271.1	267.3	2.8	10.5		B_g
	13	198.2	195.3	2.6	6.7	A_g	
*	14	191.4	190.0	1.8	5.2		B_g
	15	167.2	164.5	1.5	5.5		B_g
	16	149.0	146.3	1.0	5.2		B_g
	17	126.0	123.2	2.6	4.3	A_g	
	18	92.3	91.5	1.5	3.8		B_g

[a]Linewidths calculated assuming the convolution of two Gaussians.

TABLE III. Symmetry and frequency of internal modes at room temperature.

Symmetry	Internal modes in $ZnWO_4$ (cm^{-1})	WO_6 (cm^{-1})	Symmetry
A_g	907	817	$\nu_1(A_{1g})$
B_g	786	680	
A_g	709		$\nu_2(E_g)$
A_g	407		$\nu_3(T_{2g})$
A_g	342	444	
B_g	190		

RESULTS AND DISCUSSION

In a 90° scattering geometry, there are six independent orientations in the case of C_{2h} point-group symmetry. However, in order to check the results, spectra were obtained at 14 and 292 K in 12 different orientations, and every 25 K in the range between 14 and 292 K in 9 different orientations.

Figures 2 and 3 show typical spectra in orientations where only A_g and B_g modes are expected, respectively. Although all Raman bands are strongly polarized, the strongest A_g bands show weakly in the spectra for the B_g modes, and vice versa. The Raman frequencies obtained at 14 and 292 K in the $Y(X,X)Z$ and $X(Z,X)Y$ orientations are listed in Table II, with their mode symmetries.

In general, the internal vibrations of a tightly bound group of atoms have higher frequencies than the vibrations in which the more loosely bound groups vibrate against each other. However, in the case of $ZnWO_4$, the WO_6 octahedra share oxygen atoms and it is more difficult to clearly differentiate between internal and external vibrational modes. So, there may be considerable overlap in the frequency range for the two types of vibrations. We may, however, be able to assign the internal modes on the basis of the temperature dependence of the frequencies. In fact, the modes indicated by asterisks in Table II have nearly the same frequencies at 14 and 292 K, and are thus assigned to internal vibrations of the WO_6 octahedra. Notice that there are 4 A_g and 2 B_g modes assigned to the internal vibrations, in agreement with the group-theoretical analysis. Also notice that the remaining modes have frequencies that decrease more rapidly with temperature, with the exception of mode 4, which has an anomalous temperature dependence.

The modes assigned to internal vibrations of the WO_6 octahedra are again listed in Table III and correlated to the vibrations of the isolated regular octahedron. Typical frequencies quoted for the WO_6 regular octahedron[11] and the frequencies observed in the present study are also listed. The A_{1g} mode (symmetric stretch) of the regular octahedron has A_g symmetry in the crystal. It is assigned to the A_g mode observed near 907 cm^{-1} since, as is the case of the regular octahedron, the symmetric stretch is expected to have the highest frequency of all the internal modes. The E_g mode (asymmetric stretch) of the regular octahedron splits into A_g+B_g by the crystal field. Again, these modes are expected to have frequencies that are higher than those of the bending mode (T_{2g}) of the regular octahedron. The obvious choices are the B_g and A_g modes observed near 786 and 709 cm^{-1}, respectively. The remaining modes 2 A_g+B_g with frequencies of 407, 342, and 190 cm^{-1} are assigned to the T_{2g} mode of the regular octahedron.

Although the internal modes change little with temperature, they do change. Tables IV and V list their frequencies and linewidths at various temperatures between 14 and 292 K. Anharmonic terms in the crystal potential energy are responsible for shifts in the mode frequencies. The shifts in frequency with temperature are not only due to the anharmonic coupling of the phonons, but also to the changes in crystal volume V associated with thermal expansion.[12,13] If the frequency of the ith mode ω_i is a function of temperature T and pressure P, one may write[14]

$$\left[\frac{\partial \ln\omega_i}{\partial T}\right]_P = \alpha\gamma_i + \left[\frac{\partial \ln\omega_i}{\partial T}\right]_V , \quad (1)$$

where α is the thermal expansion coefficient and γ_i is the Grüneisen parameter of the ith mode.

There is no published data on α and γ_i for $ZnWO_4$. However, the Grüneisen parameters of internal modes in molecular crystals are usually 2 orders of magnitude smaller than those of the external modes.[15,16] Assuming

TABLE IV. Frequencies of internal modes (cm^{-1}) at various temperature.

T (K)	Mode 1	Mode 2	Mode 3	Mode 7	Mode 9	Mode 14
14	907.5	787.3	709.0	408.0	342.5	191.4
30	907.5	787.5	709.0	408.0	342.5	191.3
50	907.5	787.3	709.0	408.0	342.5	191.3
75	907.2	787.1	709.0	408.0	342.5	191.4
100	907.2	787.2	709.0	408.0	342.4	191.2
125	907.2	786.9	709.1	408.0	342.4	190.9
150	907.2	786.8	709.1	408.0	342.4	190.8
175	907.1	786.6	709.1	407.6	342.3	190.7
200	906.9	786.6	709.1	407.5	342.1	190.7
225	907.2	786.2	709.2	407.4	342.2	190.5
250	907.0	786.4	709.6	407.1	342.0	190.5
275	906.8	785.8	708.8	407.1	341.9	190.2
292	906.8	785.9	709.1	406.9	341.8	190.0

TABLE V. Linewidths of internal modes in cm^{-1} at various temperatures, obtained assuming a convolution of two Gaussians (Lorentzians).

T (K)	Mode 1	Mode 2	Mode 3	Mode 7	Mode 9	Mode 14
14	5.2 (2.1)	6.0 (2.7)	6.6 (3.1)	3.6 (1.1)	3.6 (1.1)	1.8 (0.3)
30	5.2 (2.1)	6.4 (3.0)	6.6 (3.1)	3.6 (1.1)	4.0 (1.3)	2.4 (0.5)
50	5.2 (2.1)	6.7 (3.2)	7.1 (3.5)	3.6 (1.1)	4.0 (1.3)	2.6 (0.6)
75	5.5 (2.3)	7.1 (3.5)	6.6 (3.1)	4.0 (1.3)	4.6 (1.7)	2.8 (0.7)
100	5.8 (2.5)	7.9 (4.2)	7.2 (3.6)	4.5 (1.6)	4.9 (1.9)	2.6 (0.6)
125	6.2 (2.8)	8.4 (4.6)	8.3 (4.5)	5.2 (2.1)	5.1 (2.0)	3.6 (1.1)
150	6.2 (2.8)	9.4 (5.4)	8.4 (4.6)	5.2 (2.1)	5.9 (2.6)	4.0 (1.3)
175	6.4 (3.0)	9.9 (5.9)	9.4 (5.4)	5.2 (2.1)	6.4 (3.0)	4.1 (1.4)
200	6.9 (3.4)	10.8 (6.2)	9.8 (5.8)	5.9 (2.6)	7.1 (3.5)	4.0 (1.3)
225	6.9 (3.4)	12.5 (8.2)	10.4 (6.3)	7.2 (3.6)	7.8 (4.1)	4.5 (1.6)
250	7.4 (3.8)	13.5 (9.1)	11.9 (7.7)	9.0 (5.1)	8.4 (4.6)	4.9 (1.9)
275	8.1 (4.3)	15.1 (10.6)	12.3 (8.0)	11.3 (7.1)	9.4 (5.4)	5.3 (2.2)
292	8.3 (4.5)	15.1 (10.6)	12.9 (8.6)	10.2 (6.1)	9.6 (5.6)	5.2 (2.1)

that the first term in Eq. (1) will be small for the internal modes of $ZnWO_4$, then the frequency shifts are mainly due to the second term, which is a direct result of anharmonic interactions and is present even in a solid held at a constant volume.

A perturbation treatment starting from conventional lattice dynamics can be used to calculate the anharmonic contributions in the case of small vibrational amplitudes.[17] Usually, cubic and quartic anharmonic terms are considered and the total energy is then calculated in second-order perturbation. The resulting correction to the harmonic energy is called the anharmonic self-energy. This self-energy is complex, the real part representing the shift in the Raman frequency and the imaginary part is related to the width of the Raman line. In second-order perturbation, both cubic and quartic anharmonic terms contribute to the frequency shift while only cubic terms contribute to the linewidth.

If a mode frequency ω interacts predominantly with only one other mode of frequency ω', then ω is given by[18]

$$\omega=\omega_0+An(\omega') , \tag{2}$$

where ω_0 is the mode frequency at 0 K, A is a temperature-independent term that depends on the strength of the anharmonic interaction, and $n(\omega')$ is the Bose-Einstein occupation number

$$n(\omega')=\frac{1}{e^{hc\omega'/k_BT}-1} , \tag{3}$$

where h is Planck's constant, c is the speed of light, k_B is Boltzmann's constant, and T is absolute temperature.

The observed mode frequencies from Table IV were fitted to the temperature dependence given by Eq. (2), with the exception of mode 3, which has a frequency that remains constant with temperature within the experimental uncertainty. The best fit in the case of mode 14 is shown by the solid line in Fig. 4. The resulting parameters for four of the internal modes are listed in Table VI. The values of ω' obtained for a particular mode need not be the same as the frequency of another mode since the observed phonon is likely to be interacting with many others, in which case ω' represents the frequency of an "average" phonon with which the observed phonon is interacting. The value of ω' obtained for mode 1 was nearly zero. This indicates that this mode, which corresponds to the symmetric stretch of the WO_6 octahedra, is only interacting with acoustic phonons. For small ω', the occupation number $n(\omega')$ and, hence, the frequency ω given

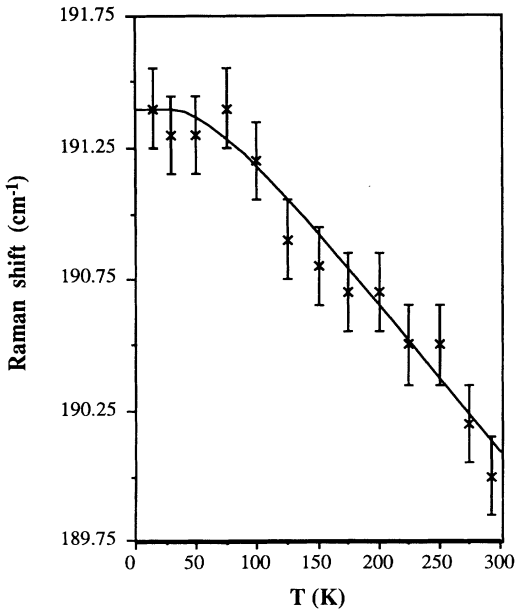

FIG. 4. Temperature dependence of the frequency of mode 14. The crosses are the experimental points and the solid line is the best fit to Eq. (2).

TABLE VI. Best values of the parameters in Eq. (2) for four of the internal modes.

Mode	ω_0 (cm^{-1})	A	ω' (cm^{-1})
2	787.4	−1.051	107.9
7	408.0	−5.112	344.2
9	342.5	−2.340	304.7
14	191.4	−1.005	118.6

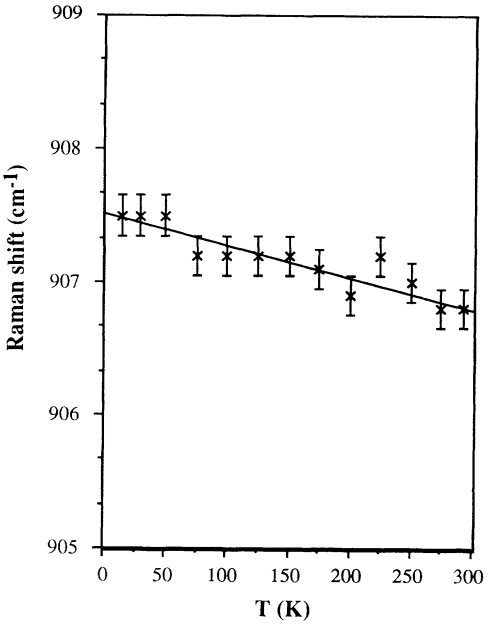

FIG. 5. Temperature dependence of the frequency of mode 1. The crosses are the experimental points and the solid line is the best fit to a straight line.

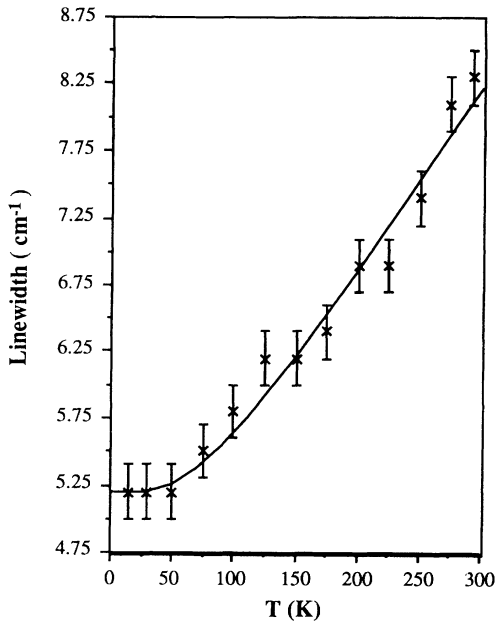

FIG. 6. Temperature dependence of the linewidth of mode 1. The crosses are experimental points and the solid line is the best fit to Eq. (4).

by Eq. (2) become linear with temperature. Indeed, Fig. 5 shows the data points for mode 1 and the straight line obtained with a least-squares fit.

The instrumental profile in the present study is Gaussian and, if the true line shape is Lorentzian, the observed line shape should be a Voigt profile. The method of Asthana and Kiefer[19] was used for the deconvolution of the Lorentzian linewidth of the internal modes. In this method, the Lorentzian character of the observed line is determined from its shape. Then, a parameter y, which gives the ratio of the true linewidth to the instrumental linewidth, is determined from a table.

The above method resulted in a linewidth for the internal mode near 907 cm^{-1} that increases monotonically with temperature. However, inconsistent results were obtained for the other internal modes, with a scatter in the calculated values that is as large as the linewidths. The authors believe that these results are mainly due to two factors. First, a signal-to-noise ratio of 100 or higher seems necessary to be able to fit an observed Raman line to a Voigt profile.[20] This is satisfied in the present study only in the case of the internal mode near 907 cm^{-1}. Second, the parameter y tabulated in Ref. 19 is extremely sensitive to small changes in the observed line shape. As a consequence, large changes in the calculated linewidth are obtained for changes in the observed linewidth as small as 0.02 cm^{-1}, which is very small compared to the present instrumental resolution. A resolution less than 0.01 cm^{-1} can be achieved by coupling the Raman spectrometer to a Fabrey-Pérot interferometer.[21]

For the present study, however, the authors have concluded that a deconvolution of a Voigt profile does not given meaningful results. Indeed, the linewidths were calculated assuming a convolution of either two Gaussians or two Lorentzians, and the true linewidths will have values between those extremes. The results are given in Table V.

In second-order perturbation, the temperature dependence of the linewidth arises only through cubic anharmonic interactions corresponding to decay and combination processes. The expression for the linewidth then contains a sum of terms, each representing a decay or combination process. However, the best fits to the data for each mode resulted in a dominant term in the sum. For five of the six internal modes, this single term corresponds to a combination of the observed phonon with another phonon of frequency ω' to create a third excitation of frequency ω'', where, by conservation of energy $\omega''=\omega+\omega'$. In that case, the linewidth Γ of the observed mode is given by

$$\Gamma=\Gamma_0+B[n(\omega')-n(\omega+\omega')] , \quad (4)$$

where Γ_0 is the linewidth at 0 K and B is a temperature-independent factor that depends on the strength of the cubic anharmonic interaction.

Figure 6 shows the linewidth of mode 1 obtained from the deconvolution of two Gaussians and the best fit to Eq. (4). The resulting parameters for five of the internal

TABLE VII. Parameters obtained from a fit to Eq. (4) of the linewidths obtained from the deconvolution of two Gaussians (Lorentzians).

Mode	ω (cm^{-1})	ω' (cm^{-1})	ω'' (cm^{-1})
1	907	141 (171)	1048 (1078)
2	786	170 (192)	957 (979)
3	709	198 (215)	907 (924)
7	407	450 (531)	858 (939)
9	342	171 (229)	513 (571)

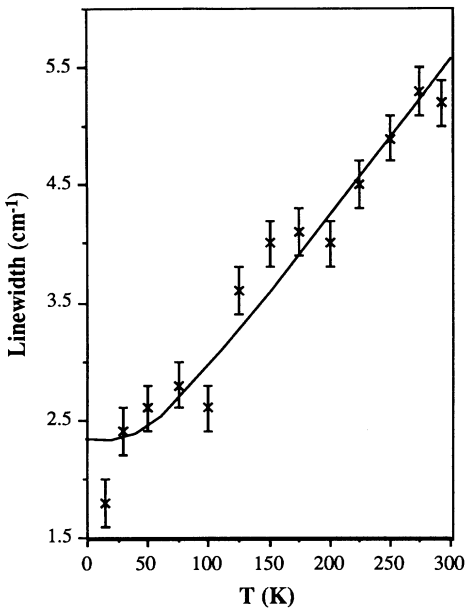

FIG. 7. Temperature dependence of the linewidth of mode 14. The crosses are the experimental points and the solid line is the best fit to Eq. (5).

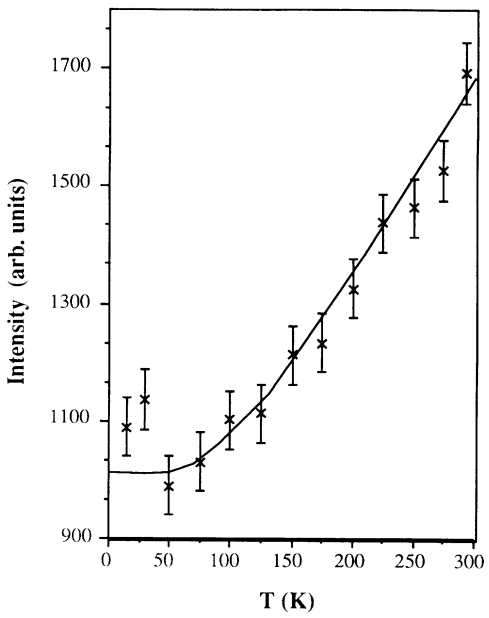

FIG. 8. Temperature dependence of the peak intensity of mode 14. The crosses are the experimental points and the solid line is the best fit to Eq. (6).

modes are listed on Table VII. The two sets of linewidths in Table V were used, resulting in values of ω' and ω'' that differ by an average of 10%. Using the true linewidths should result in values of ω' and ω'' that are between those listed in the table. The ranges of values obtained from ω' and ω'' for each of the five internal modes contain at least one of the observed Raman frequencies, except for the values of ω'' obtained for modes 1 and 2 (compare Tables II and VII). However, the Raman frequencies correspond to long-wavelength excitations and the excitations with frequencies ω' and ω'' are not restricted to wave vectors near the center of the Brillouin zone.

The linewidth of mode 14 could not be fitted to Eq. (4), but was well represented by the equation

$$\Gamma = C + D\left[2n\left[\frac{\omega}{2}\right]+1\right], \tag{5}$$

where C and D are constants. This equation is obtained by assuming that the observed phonon decays into two phonons of equal energy and opposite momenta.[22] The observed linewidth of mode 14 was fitted to Eq. (5) and shown in Fig. 7, resulting in values of $C=1.3847$ cm^{-1} and $D=0.9386$ cm^{-1}.

Besides having a linewidth with a temperature dependence resulting from a decay process, mode 14 is different from the other internal modes in that its peak intensity increases with temperature. In fact, in the harmonic approximation, the Raman intensity is proportional to a thermal factor that increases with temperature, so that it is given by[23,24]

$$I = I_0[n(\omega)+1], \tag{6}$$

where I_0 is temperature independent. The observed intensity and the best fit to Eq. (6) for mode 14 are shown in Fig. 8. Note that ω is fixed, which is the frequency of mode 14, so that I_0 is the only adjustable parameter. For the other internal modes, there is an additional temperature dependent factor due to anharmonicity and the intensities could not be fitted to Eq. (6).

In summary, the 18 vibrational modes, 8 A_g+10 B_g, expected from group-theoretical analysis, have been observed in the polarized Raman spectra of $ZnWO_4$. The six internal modes of WO_6 octahedra have been identified and correlated to the vibrational modes of the isolated regular octahedron. These internal modes have frequencies which are weakly temperature dependent. The temperature dependence of the frequencies and linewidths of the internal modes can be understood in terms of anharmonic interactions.

ACKNOWLEDGMENT

The authors wish to thank Professor H. Z. Cummins for helpful discussions.

*Present address: Department of Physics, Beijing Television University, Beijing, China.

[1]T. Oi, K. Takagi, and T. Fukazawa, Appl. Phys. Lett. **36**, 278 (1980).

[2]B. C. Grabmaier, IEEE Trans. Nucl. Sci. **NS-31**, 372 (1984).

[3]W. Kolbe, K. Petermann, and G. Huber, IEEE J. Quant. Electron. **QE-21**, 1596 (1985).

[4]Y. V. Pisarevskii, I. M. Silvestrova, R. Voszka, A. Péter, I.

Földvári, and J. Janszky, Phys. Status Solidi A **107**, 161 (1988).
[5]J. G. Rushbrooke and R. E. Ansorge, Nucl. Instrum. Methods Phys. Res. A **280**, 83 (1989).
[6]H. Wang, Y. Liu, Y. D. Zhou, G. Chen, T. Zhou, J. H. Wang, and B. Q. Hu, Acta Phys. Sin. **38**, 670 (1989).
[7]H. Wang, Y. Liu, Y. D. Zhou, G. Chen, B. Q. Hu, and B. Y. Gu, Acta Phys. Sin. **37**, 43 (1988).
[8]O. S. Filipenko, E. A. Pobedimskaya, and N. V. Belov, Kristallografiya **13**, 163 (1968).
[9]O. S. Filipenko, E. A. Pobedimskaya, V. I. Ponomarev, and N. V. Belov, Kristallografiya **13**, 1073 (1968).
[10]Y. D. Zhou, G. Q. Liu, and S. L. Jiang, J. Chin. Ceram. Soc. **14**, 479 (1986).
[11]P. Ahamad, L. Dixit, and N. K. Sanyal, Indian J. Appl. Phys. **12**, 489 (1974).
[12]R. A. Cowley, Adv. Phys. **12**, 421 (1963).
[13]F. Gervais, B. Piriou, and F. Cabannes, Phys. Status Solidi B **51**, 701 (1972).
[14]P. T. T. Wong, J. Chem. Phys. **63**, 5108 (1975).
[15]D. M. Adams, A. C. Shaw, G. A. Mackenzie, and G. S. Pawley, J. Phys. Chem. Solids **41**, 149 (1980).
[16]T. E. Jenkins, J. Phys. C **19**, 1065 (1986).
[17]D. C. Wallace, *Thermodynamics of Crystals* (Wiley, New York, 1972).
[18]F. D. Medina and W. B. Daniels, J. Chem. Phys. **64**, 150 (1976).
[19]B. P. Asthana and W. Kiefer, Appl. Spectros. **36**, 250 (1982).
[20]J. Menéndez and M. Cardona, Phys. Rev. B **29**, 2051 (1984).
[21]R. Ouillon, C. Tarc, J. P. Lemaistre, and P. Ranson, J. Chem. Phys. **93**, 3005 (1990).
[22]P. G. Klemens, Phys. Rev. B **11**, 3206 (1975).
[23]R. Loudon, Adv. Phys. **13**, 423 (1964).
[24]V. A. Haisler, V. M. Zaletin, and A. F. Kravchenko, Phys. Status Solidi B **125**, K103 (1984).